

An experimental investigation on the effects of exponential window and impact force level on harmonic reduction in impact-synchronous modal analysis[†]

Ong Zhi Chao^{1,*}, Lim Hong Cheet¹, Khoo Shin Yee¹, Abdul Ghaffar Abdul Rahman² and Zubaidah Ismail³

¹Mechanical Engineering Department, Faculty of Engineering, University of Malaya, 50603 Kuala Lumpur, Malaysia

²Faculty of Mechanical Engineering, University Malaysia Pahang, 26600 Pekan, Pahang Darul Makmur, Malaysia

³Civil Engineering Department, Faculty of Engineering, University of Malaya, 50603 Kuala Lumpur, Malaysia

(Manuscript Received December 23, 2015; Revised March 30, 2016; Accepted April 15, 2016)

Abstract

A novel method called Impact-synchronous modal analysis (ISMA) was proposed previously which allows modal testing to be performed during operation. This technique focuses on signal processing of the upstream data to provide cleaner Frequency response function (FRF) estimation prior to modal extraction. Two important parameters, i.e., windowing function and impact force level were identified and their effect on the effectiveness of this technique were experimentally investigated. When performing modal testing during running condition, the cyclic loads signals are dominant in the measured response for the entire time history. Exponential window is effectively in minimizing leakage and attenuating signals of non-synchronous running speed, its harmonics and noises to zero at the end of each time record window block. Besides, with the information of the calculated cyclic force, suitable amount of impact force to be applied on the system could be decided prior to performing ISMA. Maximum allowable impact force could be determined from non-linearity test using coherence function. By applying higher impact forces than the cyclic loads along with an ideal decay rate in ISMA, harmonic reduction is significantly achieved in FRF estimation. Subsequently, the dynamic characteristics of the system are successfully extracted from a cleaner FRF and the results obtained are comparable with Experimental modal analysis (EMA).

Keywords: Exponential window; Frequency response function estimation; Force identification; Harmonic reduction; Impact-synchronous modal analysis; Modal testing

1. Introduction

Experimental modal analysis (EMA) requires the system to be in complete ‘shutdown’ mode. In other words, there should be no unaccounted excitation force induced into the system. Measurable impact or random forces are used to excite the system. Various curve-fitting algorithms as exemplified by several workers [1-5] are then used to extract the three modal parameters. In applications, the extracted modal parameters from EMA have been widely used to detect damage on beams and beam-like structures [6-8] as well as rotor systems [9].

Operational modal analysis (OMA) has been introduced and various studies have been conducted in order to perform modal analysis while the machines are running. Some examples include the Natural excitation technique (NExT) which is a method of modal testing that allows structures to be tested in their ambient environments [10]. The time domain identification methods [11-14], the frequency domain identification methods [15-18] and analyses with phase and frequency cor-

rections methods [19-21] are the identification techniques used in OMA. In OMA, structural modal parameters can be computed without knowing the input excitation to the system. It is therefore a valuable tool to analyse structures subjected to excitation generated by their own operation. In practical situations where the system cannot have a complete ‘shutdown’ or the structure is too large to response to ‘artificial’ excitation, OMA is sought. OMA holds certain advantages over EMA for its practicality and easiness to carry out. Also, it performs the analysis while the system is running and the measured responses are representative of the actual operating conditions of the structure. However, the lack of knowledge of the input forces does affect the parameters extracted. For example, mode shapes obtained from OMA cannot be normalised accurately, subsequently affecting the mathematical models.

Over the years, as the part of the effort to improve the estimation accuracy in OMA and EMA, the focus was mainly on the development of modal identification algorithms [1-5, 15-22]. Relatively less effort was put into improving the digital signal processing aspects, especially upstream of the collected data. Impact-synchronous modal analysis (ISMA) [23, 24] has the advantages of the OMA and EMA combined. It carries out

*Corresponding author. Tel.: +60 3 7967 6815, Fax.: +60 3 79675317

E-mail address: zhichao83@gmail.com; alexongzc@um.edu.my

[†]Recommended by Editor Yeon June Kang

© KSME & Springer 2016

the analysis while the system is in operation and at the same time is able to provide the actual input forces in the transfer functions, hence, allowing for better modal extractions. This novel technique can be applied in both rotor and structural dynamic systems to obtain the dynamic characteristics of structures without disturbing the operations. This is very crucial for the industrial plants especially those high downtime cost rotating machinery. In petrochemical plants, the downtime cost alone can go up to USD 6000 to 90000 per hour.

In ISMA, when the analysis is performed while machine is in running condition, all the responses contributed by the unaccounted forces are filtered out in the time domain, leaving only the responses triggered due to the impact hammer. This is achieved by utilizing the Impact-synchronous time averaging (ISTA) [23, 25, 26] prior to performing the Fast Fourier transform (FFT) operation. The process of modal parameters extraction follows the EMA procedures. In ISTA, block averaging is performed on the time block of both the force and response. Each time block is initiated by the impulse generated from the force trace of the impact hammer. Taking sufficient number of averages, it filters out most of the signatures of non-synchronous in frequency and phase to the impact time block. The periodic responses of cyclic loads and ambient excitations are no more in the same phase position for every time block acquired. Averaging process of repetitive impact will slowly diminish these components hence leaving behind only the structure's response to impulses which are synchronous to the repetitive impact force. Previous research have discussed on the importance of ISTA in removing dominant cyclic load components and its suitability to be used during operation as compared to spectral averaging technique. Better coherence function using ISTA could be obtained and this will lead to unnecessary rejection of good FRF estimation [24].

In real practice, the harmonics are originate from the operating system, e.g., ventilation systems, turbines and generators [27, 28]. The amplitude of the harmonics is very high and dominates the total responses captured. This could limit the effectiveness of the ISMA when performing on system with dominant operating cyclic loads. If the harmonics are close to the natural frequencies of a system, then the identification of the neighbouring mode becomes erroneous and algorithm may tend to indicate harmonic mode as a structural mode. It is also seen that if the amplitude of the harmonics is dominant then the harmonics cannot be eliminated from the response. Hence, the modal identification procedures might lose their robustness and lead to inaccurate identified modal parameters.

Generally, the effectiveness of ISMA is governed by four important parameters; (1) number of averages; (2) phase synchronization between acceleration response and response due to cyclic load; (3) windowing function and (4) impact force level [25]. To achieve prominent results in ISMA, synchronization of impact frequency and operating speed of the system should be avoided. This can be done by performing the impact randomly using impact hammer and increasing the number of averages to filter out the non-synchronous components if the

impact frequency is not synchronized with the operating speed of the system. Previous research has experimentally demonstrated the effectiveness of averages taken in the determination of dynamic characteristics of a motor driven structure. By increasing the number of averages, the responses due to cyclic load components were greatly removed leaving only the impulse responses only. In this experimental investigation, random impacts by the conventional impact hammer were applied. However, it was found that at operating speeds that coincided with the natural modes where cyclic load component is the most dominant due to resonance, ISMA required a high number of impacts to determine the dynamic characteristics of the system [29]. This has led to the practicality and effectiveness of the technique in question.

Thus, the studies should focus on the effect of other parameters, i.e., windowing function and impact force level. These parameters were identified to be equally important as number of averages in further enhancing the effectiveness of ISMA. This research gap has initiated the needs of studying the effects of exponential windowing function and impact force on the harmonic reduction in FRF estimation in order to further enhance the ISMA. The study involves two stages of experimental investigations. In the first stage, different levels of exponential windows are applied in the acquired time response signals to study the effectiveness in minimizing leakage and filtering out all the responses contributed by unaccounted forces. In second stage, a force screening assessment is then performed along with the optimum decay rate of exponential window determined from the first stage in the effort of investigating the effect of impact force level associated with dominant cyclic load effect in reducing the harmonics during ISMA. Optimum decay rate of exponential window and impact force level could yield a better FRF estimation which will lead to accurate identification of dynamic characteristics.

2. Mathematical background

2.1 Exponential windowing function

The general form of the response of a structure being excited by an impact is:

$$y(t) = \sum_{k=1}^n [R_k e^{-\sigma_k t} \sin(w_k t)] \quad (1)$$

where n is the number of modes in the frequency range being excited, R_k is the constant for mode k , σ_k is the decay rate for mode k and w_k is the damped natural frequency of mode k .

When an exponential window is applied, the response time history becomes:

$$y'(t) = e^{-\sigma_w t} \sum_{k=1}^n [R_k e^{-\sigma_k t} \sin(w_k t)] \quad (2)$$

Rearranging Eq. (2) and reduce to the following f

$$y'(t) = \sum_{k=1}^n [R_k e^{-\sigma_k t} \sin(w_k t)] \tag{3}$$

The apparent damping for mode k is:

$$\sigma_k' = \sigma_0 + \sigma_k \tag{4}$$

From the above equations, it is noted that the exponential window just adds a constant amount of damping σ_0 to each mode of vibration in the FRF estimation. The modal analysis system processes the set of FRF estimation and the apparent damping σ_k' is estimated during the curve fitting process. Thus, the actual damping of the mode, σ_k could be calculated using the following equation:

$$\sigma_k = \sigma_k' - \sigma_0 \tag{5}$$

2.2 Force identification

The general solution of the linear forced vibration system can be expressed in frequency domain as following:

$$\left\{ \ddot{X}(\omega) \right\}_{n \times 1} = [H(\omega)]_{n \times n} \left\{ Q(\omega) \right\}_{n \times 1} \tag{6}$$

where $[H(\omega)]$ is an n x n square matrix of FRF estimation which represents the dynamic characteristic of a system. It is a transfer function and named as accelerance or inertance. $\{\ddot{X}(\omega)\}$ and $[Q(\omega)]$ are n x 1 frequency varying vectors of accelerations and forces. These functions are complex function which is transformable from Cartesian coordinate to polar coordinate and vice versa.

Eq. (6) can be rewritten and reduced to the following form

$$\begin{Bmatrix} Q_{1x} \\ Q_{1y} \\ Q_{1z} \end{Bmatrix} = inv \begin{bmatrix} A_{1x1x} & H_{1x1y} & H_{1x1z} \\ A_{1y1x} & H_{1y1y} & H_{1y1z} \\ H_{1z1x} & H_{1z1y} & H_{1z1z} \end{bmatrix} \begin{Bmatrix} \ddot{X}_{1x} \\ \ddot{X}_{1y} \\ \ddot{X}_{1z} \end{Bmatrix} \tag{7}$$

where inv is the direct inverse method.

In the past years, researchers have developed many methods to improve the accuracy of force identification [30-33]. With pseudo-inverse method, force magnitude for a specific direction at the known single location can be calculated. For example, the single column of FRF estimation matrix at force DOF, Z direction is used in force determination procedure, then unknown excitation forces in Z axes will be calculated. This is shown in Eq. (8).

$$\left\{ Q_{1z} \right\} = inv \begin{bmatrix} H_{1x1z} \\ H_{1y1z} \\ H_{1z1z} \end{bmatrix} \begin{Bmatrix} \ddot{X}_{1x} \\ \ddot{X}_{1y} \\ \ddot{X}_{1z} \end{Bmatrix} \tag{8}$$

where pinv $[H_{ij}]$ is the pseudo-inverse of the FRF estimation.

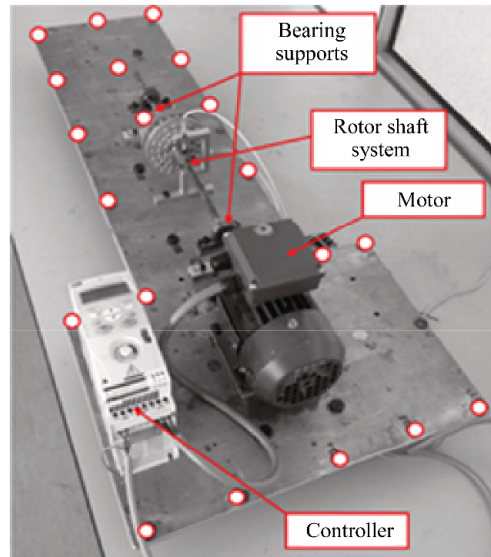


Fig. 1. Motor-driven test rig.

The FRF estimation is formed by response data at DOF I and force data at DOF J.

$$pinv[H_{ij}] = inv \{ [H_{ij}]^h [H_{ij}] \} [H_{ij}]^h \tag{9}$$

where inv is the direct inverse method. \bullet^h is the complex conjugate transpose of a matrix (Hermitian matrix).

2.3 Non-linearity test

Coherence is a direct measure of how the excitation is linearly related to the structural response [34-36]. Coherence function, γ^2 is defined as following.

$$\gamma^2 = \frac{|S_{xq}(\omega)|^2}{S_{qq}(\omega) \cdot S_{xx}(\omega)} \tag{10}$$

where $S_{qq}(\omega)$ is the auto power spectrum for the excitation, $S_{xx}(\omega)$ is the auto power spectrum for the response and $S_{xq}(\omega)$ is the cross power spectrum between excitation and response. Coherence near to 1 indicates that the measurements are believable and that noise and non-linear effects are not significant. If the coherence is near zero, it means that the measurements should be viewed with great suspicion [37].

3. Measurement procedures and instrumentation

The test rig used in this study consists of a motor coupled to rotor shaft system as shown in Fig. 1. The instrumentation and procedures used in ISMA was the same as in EMA using fixed excitation roving responses method. The only difference was that the averaging techniques allowed the procedure to be carried while the machine was in operation. Rahman et al.

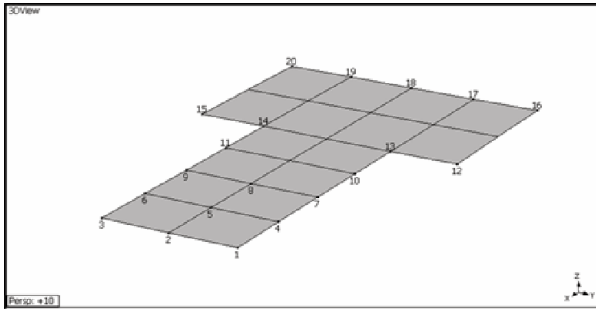


Fig. 2. Structural wire-mesh model of motor-driven test rig.

[24] explained the complete experimental procedures of ISMA.

An impact hammer equipped with a force transducer was used to strike the structure and an accelerometer measured the structure's response vibration. The force transducer was connected to one input channel of the analyser and the tri-axial response accelerometer was connected to the second, third and fourth channels of the data acquisition system. The sampling rate used was 2048 samples/sec with the block size of 4096. This yields frequency resolutions of 0.5 Hz and 2 seconds of time record length to capture every response signal due to impact.

EMA was conducted with five averages or impacts and formed as a benchmark data. In ISMA, the system was set to operate at two different speed modes, i.e., 20 Hz and 30 Hz, with average of 250 impacts were taken. High number averages at 250 was taken and fixed in order to minimise the effect of number of averages in ISMA. Decay rate of exponential window was manipulated at different operating conditions to study the effect of the windowing functions in ISMA. The signals were averaged and processed by the EMA and ISMA application programmes developed using virtual instruments software called DASYLab to generate the Frequency response functions (FRFs) estimation and coherence functions. The modal extraction techniques applied to EMA could also be applied in ISMA. Fig. 2 shows a three-dimensional structural model that represents the base plate used in this study. It consists of a series of points with Cartesian coordinate connected together using straight lines to form surfaces using a modal analysis software called ME'scope. The displayed point numbers show the measurement locations as in the actual base plate. This model was used to display the mode shapes of the rig from the acquired data. Lastly, the modal parameters obtained using ISMA at different decay rate on exponential windowing function followed by impact force (low and high) during operating conditions were compared with the benchmark and the consistency of the mode shapes were shown in MAC values.

To determine the level of impacts applied on the structure, cyclic load should be calculated in advance. The procedures of force calculation are as following, (1) decide the impact location; point 1 was selected in this study, (2) excite vertical (Z) axis and measure the FRF estimation using EMA at point 1 in

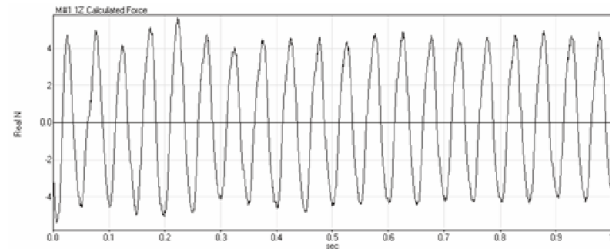


Fig. 3. Calculated cyclic force in time domain of point 1 at 20 Hz z-axis.

three directions respectively, (3) measure the acceleration time responses of point 1 in Z axis at operating speeds of 20 Hz and 30 Hz accordingly and (4) perform direct inverse force identification method in modal analysis software, ME'Scope by importing the acquired FRFs estimation and response time traces to calculate the force due to the periodic response in time domain.

In this study, only 2 different impact forces were applied on the test rig in order to investigate the effect of impacts in ISMA at three running conditions. EMA and ISMA are performed using fixed excitation roving responses method. It is worthwhile to mention that fixing impact location during ISMA would be more practical and time saving. Forces could be applied at this predefined location in three different directions where some other locations would have obstructions and inaccessible in certain directions. In addition, by fixing impact location, only a single location cyclic force is calculated and more consistent impact forces could be applied at that location. Unlike roving excitation fixed response method, cyclic force at all the locations should be calculated prior to applying correct impact force at that particular location. In this investigation, impact location was fixed and excited in vertical direction (Z axes) at point 1 with 250 averages.

To test non-linearity behaviour on a structure, small amount of force was applied during an impact test. The force level was increased accordingly. The coherence would dramatically decrease in value throughout the frequency ranges if the structure exhibits a load dependent non-linearity. This non-linearity test would determine the maximum allowable impact force that can be applied on the simulation rig.

4. Results and discussion

4.1 Force identification and non-linearity test

The calculated forces in vertical direction or Z axis are identified because this is the impact direction used in ISMA in latter stage. As shown in Fig. 3, 5 Newton of force is recorded when the test rig is operating at 20 Hz. Meanwhile, at 30 Hz, the cyclic forces has increased and achieved to maximum of 20 Newton. This calculated periodic force in time domain is shown in Fig. 4. Fig. 5 shows the result of non-linearity test. The overall coherence value starts to drop below 0.8 when impact force of 250 Newton is applied at point 1 of the test rig.

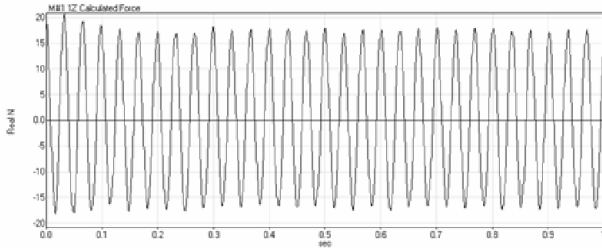


Fig. 4. Calculated cyclic force in time domain of point 1 at 30 Hz in z-axis.

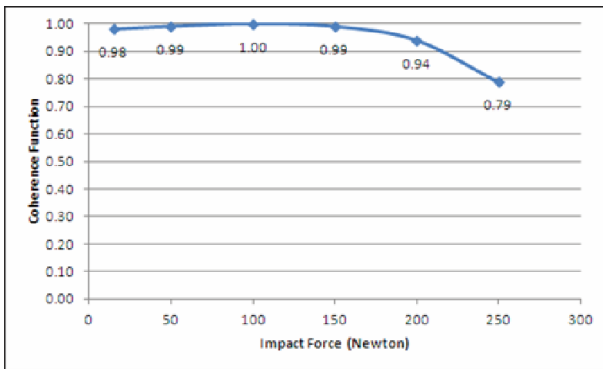


Fig. 5. Non-linearity test using coherence function.

This high impact force has caused non-linearity behaviour to the rig. In short, the maximum allowable impact force applies on this rig should not exceed 250 Newton as determined in non-linearity test. Therefore, performing ISMA with impact forces apply at point 1 should exceed 20 Newton in order to fully determine the dynamic characteristics of first three natural modes in operating conditions.

4.2 Comparison of FRFs estimation and dynamic characteristics with ISMA through signal attenuation and force screening assessment

When no exponential window is applied, it is noticed that no attenuation of response signals. At running speeds 20 Hz and 30 Hz, the response signals due to impact are contaminated by the periodic responses of cyclic loads and ambient excitation (Figs. 6(a) and 7(a)). With application of 3.0 rad/s decay rate, the response signals due to all unaccounted forces are attenuated and decayed to zero at the end of time record leaving behind only the responses due to impulsive force (Figs. 6(b) and 7(b)).

The response time history does not decay to zero in the entire time record, therefore, when transforming to frequency domain, a clean FRFs estimation cannot be obtained as compared to non-rotating condition (Figs. 8(a) and 9(a)) when there is no windowing function being applied. Figs. 8(b) and 9(b) show that with 3.0 rad/s decay rate, FRFs estimation from ISMA at 20 Hz and 30 Hz has improved prominently as compared to FRFs estimation with no exponential window. With sufficient number of averages, (i.e. 250 averages) the periodic

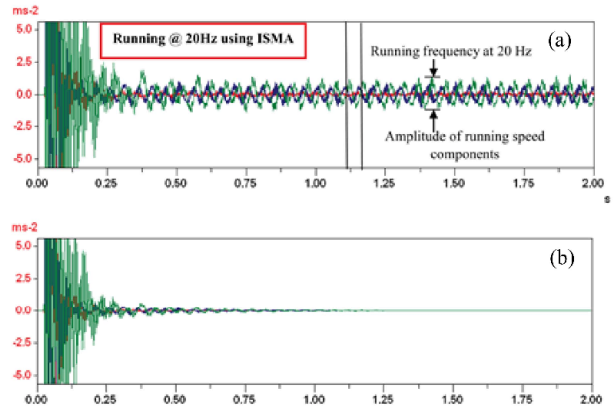


Fig. 6. Acceleration time response at operating speed of 20 Hz: (a) No exponential window; (b) 3 rad/s.

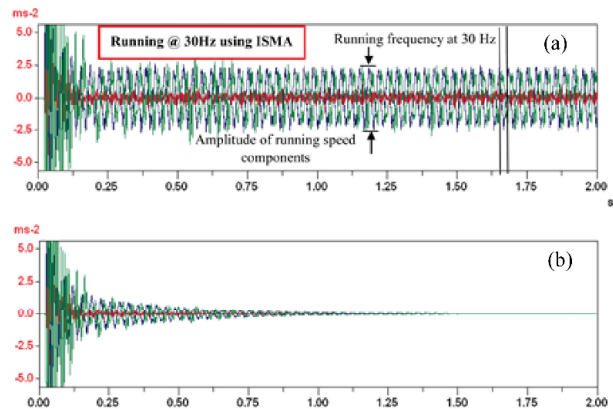


Fig. 7. Acceleration time response at operating speed of 30 Hz: (a) No exponential window; (b) 3 rad/s.

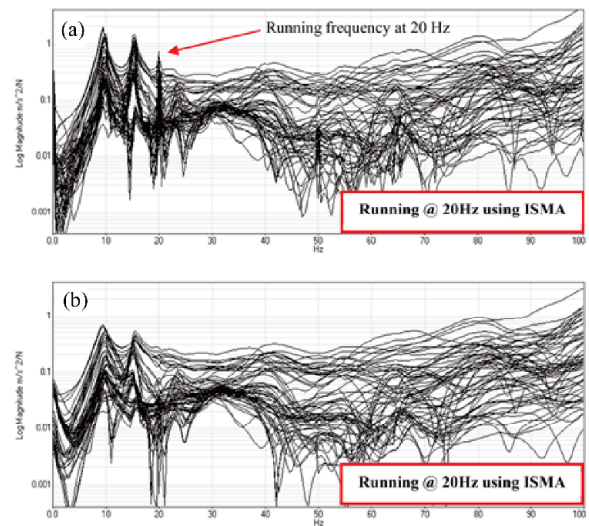


Fig. 8. FRF estimation at operating speed of 20 Hz: (a) No exponential window; (b) 3 rad/s.

responses of cyclic loads and ambient excitations are no more in the same phase position for every time block acquired and they are eventually diminished and leaving only the impulse

Table 1. Comparison of dynamic characteristics of 1st mode at different operating speeds.

Mode 1	Natural frequency (Hz)	Percentage of difference (%)	Damping, σ_k' (%)	Damping, σ_k (%)	MAC
Not running 5 averages (3.0 rad/s)	9.92	-	0.103	0.055	-
Running at 20 Hz 250 averages (0 rad/s)	9.63	3.02	0.039	0.039	0.914
Running at 20 Hz 250 averages (3.0 rad/s)	9.59	3.42	0.089	0.040	0.953
Running at 30 Hz 250 averages (0 rad/s)	9.58	3.52	0.047	0.047	0.918
Running at 30 Hz 250 averages (3.0 rad/s)	9.57	3.63	0.092	0.042	0.955

Table 2. Comparison of dynamic characteristics of 2nd mode at different operating speeds.

Mode 2	Natural frequency (Hz)	Percentage of difference (%)	Damping, σ_k' (%)	Damping, σ_k (%)	MAC
Not running 5 averages (3.0 rad/s)	15.60	-	0.043	0.013	-
Running at 20 Hz 250 averages (0 rad/s)	15.20	3.18	0.015	0.015	0.850
Running at 20 Hz 250 averages (3.0 rad/s)	15.20	3.18	0.046	0.014	0.883
Running at 30 Hz 250 averages (0 rad/s)	15.20	3.18	0.014	0.014	0.920
Running at 30 Hz 250 averages (3.0 rad/s)	15.20	3.18	0.046	0.014	0.949

Table 3. Comparison of dynamic characteristics of 3rd mode at different operating speeds.

Mode 3	Natural frequency (Hz)	Percentage of difference (%)	Damping, σ_k' (%)	Damping, σ_k (%)	MAC
Not running 5 averages (3.0 rad/s)	24.90	0.00	0.036	0.017	-
Running at 20 Hz 250 averages (0 rad/s)	23.40	6.02	0.037	0.037	0.802
Running at 20 Hz 250 averages (3.0 rad/s)	23.30	6.43	0.057	0.036	0.820
Running at 30 Hz 250 averages (0 rad/s)	23.70	4.82	0.034	0.034	0.601
Running at 30 Hz 250 averages (3.0 rad/s)	23.60	5.22	0.052	0.031	0.763

responses which are synchronous to the repetitive impact force only.

In EMA where no unaccounted forces exist, exponential window could be avoided especially on highly damped structure. However, when performing ISMA during operation, the unaccounted force components may be more dominant than impulse response. Thus, exponential window plays an important role and is necessary in all types of structure. Low damping of windowing function has not been fully attenuated the dominant periodic cyclic load signals and high damping of

exponential window has suppressed response signals of unaccounted forces together with component due to impact force. The high damping of exponential window may dampen the natural modes and this may hidden modes that are close to each other. This will cause the accuracy problem on curve fitting algorithm during modal parameters extraction.

The results obtained from ISMA at different speeds are then compared with benchmark EMA results. Mode shapes are compared using MAC value to measure the consistency of modal vectors obtained from EMA and ISMA. The results for

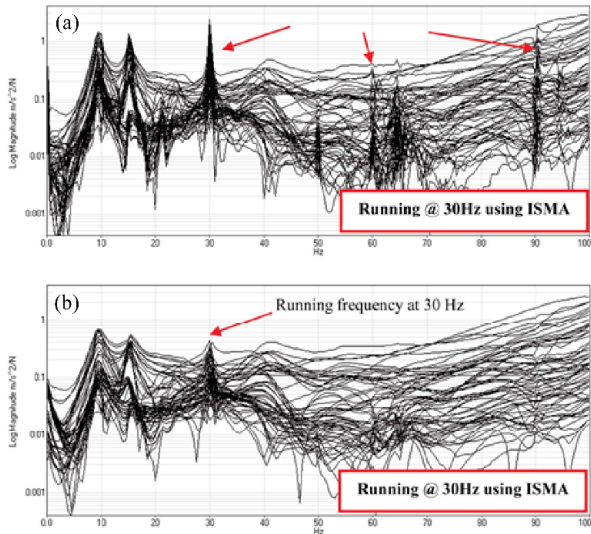


Fig. 9. FRF estimation at operating speed of 30 Hz: (a) No exponential window; (b) 3 rad/s.

the first three modes are tabulated in Tables 1-3.

At 20 Hz, when no exponential window is applied, the first three natural frequencies identified are 9.63 Hz, 15.2 Hz and 23.4 Hz with damping of 0.039%, 0.015% and 0.037%. By applying a decay rate of 3 rad/s, the identified natural frequencies for first three modes are 9.59 Hz, 15.2 Hz and 23.3 Hz with damping of 0.040%, 0.014% and 0.036%. Note that the percentage of difference between both cases is less than 7%. MAC value of above 0.9 for first mode shows good correlation between the extracted EMA and ISMA mode shapes. Second mode and third mode are considered close to the running speed of 20 Hz as compared to first mode. The operating speed sits in between these two modes. MAC values of second and third mode are below 0.9. However, better MAC is obtained with decay rate applied and consistency of the mode shape vectors between EMA and ISMA has achieved.

At 30 Hz, the vibration increases because of higher rotational or imbalance force. When no exponential window is applied, the first three natural frequencies identified are 9.58 Hz, 15.2 Hz and 23.7 Hz with damping of 0.047%, 0.014% and 0.034%. By applying a decay rate of 3 rad/s, the identified natural frequencies for first three modes are 9.57 Hz, 15.2 Hz and 23.6 Hz with damping of 0.042%, 0.014% and 0.031%. The first and second modes are far from the excitation frequency, modal parameters of these two modes in both cases are successfully extracted and well correlated with EMA with exponential window applied. Note that the percentage of difference between both cases are less than 5%. However, high speed cyclic load and ambient excitation which are near to the third mode are dominant and they cover up the third mode though decay rate of exponential windows is applied. Responses of cyclic load are more significant than the responses generated by the impact after the attenuation of the response signals with exponential window. Therefore, lower MAC (0.601) is obtained when no exponential window is

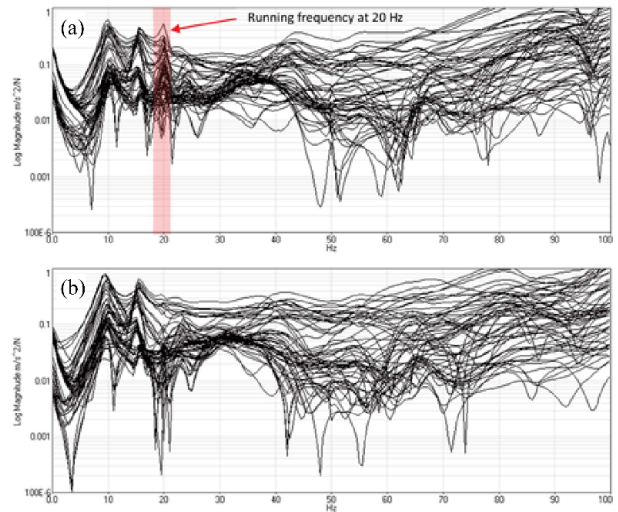


Fig. 10. Overlaid ISMA FRFs estimation running at 20 Hz with a decay rate of 3 rad/s: (a) Low impact force; (b) high impact force.

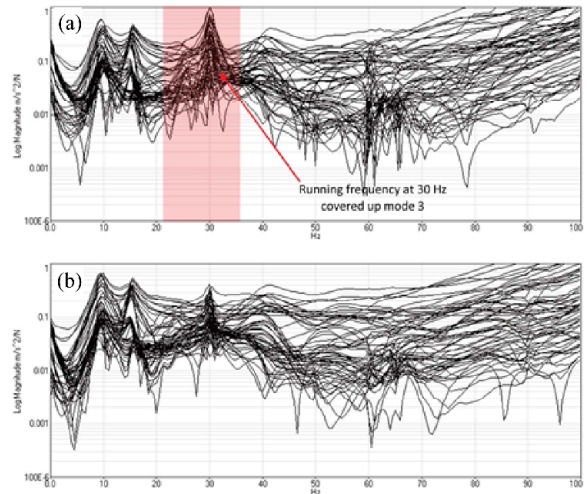


Fig. 11. Overlaid ISMA FRFs estimation running at 30 Hz with a decay rate of 3 rad/s: (a) Low impact force; (b) high impact force.

applied. It shows little correlation between mode shape of ISMA and benchmark EMA. MAC values are improved when exponential window is applied. Decay rate of 3 rad/s gives higher MAC values of 0.763. Thus, the mode shapes between EMA and ISMA achieve more than 75% correlation.

As a decay rate of 3 rad/s yields better results, the study is continued by applying low (15 Newton) and high impact force (50 Newton) in exciting the structure at the operating speed of 20 Hz and 30 Hz at a decay rate of 3 rad/s. It is observed that the comparison results are very close to both high and low impacts. Note that a higher peak of cyclic load component is observed in FRF estimation (Figs. 10(a) and 11(a)) when the impact force applied is low. However, it is worthwhile to mention that when high impact forces are applied on the rig, smoother overlaid FRFs estimation as shown in Figs. 10(b) and 11(b) are obtained for both 20 Hz and 30 Hz.

At 20 Hz, by applying high impact force, the first three

Table 4. Summary of natural frequencies and mode shapes comparison between EMA and ISMA with 20 Hz running speed with a decay rate of 3 rad/s.

Mode	Natural frequency (Hz)			Percentage of difference (%)		MAC	
	EMA	ISMA (Low impact force)	ISMA (High impact force)	EMA and ISMA (Low impact force)	EMA and ISMA (High impact force)	EMA and ISMA (Low impact force)	EMA and ISMA (High impact force)
1	9.92	9.88	9.59	0.40	3.33	0.945	0.953
2	15.6	15.4	15.2	1.28	2.56	0.927	0.883
3	24.9	23.7	23.3	4.82	6.43	0.824	0.820

Table 5. Summary of natural frequencies and mode shapes comparison between EMA and ISMA with 30 Hz running speed with a decay rate of 3 rad/s.

Mode	Natural frequency (Hz)			Percentage of difference (%)		MAC	
	EMA	ISMA (Low impact force)	ISMA (High impact force)	EMA and ISMA (Low impact force)	EMA and ISMA (High impact force)	EMA and ISMA (Low impact force)	EMA and ISMA (High impact force)
1	9.92	9.57	9.57	3.53	3.53	0.952	0.955
2	15.6	15.2	15.2	2.56	2.56	0.928	0.949
3	24.9	N/A	23.6	N/A	5.22	N/A	0.763

natural frequencies identified are 9.59 Hz, 15.2 Hz and 23.3 Hz. In addition, the first three natural frequencies identified for low impact force are 9.88 Hz, 15.4 Hz and 23.7 Hz. Generally, the percentage of difference is less than 7% for both level of impact forces applied. MAC value of above 0.9 shows good correlation between the first mode shapes extracted using ISMA and benchmark EMA for both cases. Besides, it is found that the operating speed sits in between these two modes. Thus, slightly low MAC value is obtained for the correlation of second mode between ISMA and EMA with high impact forces being applied, recorded at 0.883. The slight reduction in MAC values is due to the closeness of the second mode to operating speed at 20 Hz. Low impact force has achieved higher MAC value of 0.927. Because the third mode is less sensitive to excitation, lower MAC value of 0.820 is obtained. It shows that correlation of the mode shape vectors is acceptable. Consistency of second and third mode shapes between EMA and ISMA is established for both impact force levels.

At 30 Hz, the calculated cyclic force is registered at maximum of 20 Newton. The first three natural frequencies identified are 9.57 Hz, 15.2 Hz and 23.6 Hz for high impact force. Also, the percentage of difference is less than 6%. Since the first and second modes are far from the excitation frequency, modal parameters of these two modes are successfully extracted and well correlated with EMA. By applying high impact forces, slightly higher MAC values are obtained as compared to low impact forces, registered at 0.955 for the first mode shape correlation and 0.949 for the second mode shape correlation when benchmarked against EMA. This also indicates that the mode shapes between ISMA and EMA are well correlated. Note that lower MAC value of 0.763 is obtained for the third mode. This might be due to the amount of impact force and numbers of impacts applied are not sufficient to clean up the dominant cyclic load component and leaving the

third mode being covered up still.

Meanwhile, the first two natural frequencies identified for low impact force are 9.57 Hz and 15.2 Hz. In third mode extraction, the cyclic load at high speed and ambient excitations are dominant and cover up the mode. The responses generated by cyclic load are more significant than the responses generated by low impact at around 15 N. Thus, it is not good enough to excite and determine the less sensitive third natural mode as the mode is covered by the nearby dominating operating speed component. Thus, it will be a subject of the future investigations where higher level of impacts (but less than 250 Newton) and number of averages (more than 250 averages) can be used in ISMA to obtain more prominent results.

Tables 4 and 5 have summarized the natural frequencies and mode shapes comparison between EMA and ISMA with 20 Hz and 30 Hz running speed and a decay rate of 3 rad/s.

Generally, exponential windowing function has an important effect when performing ISMA on structures with dominant periodic responses of cyclic loads and ambient excitation. It attenuates the amplitude of the response signal exponentially from a factor of one to a small value. This is very effective especially in performing modal testing during running condition where the cyclic loads signals are dominant during the entire measured response time history. Through averaging, the exponential window performs a dual task. It eliminates or minimises leakage due to truncated response signal on a low damped structure and also filters out all the responses contributed by the unaccounted forces in a time record window block.

Besides, the impact force is another concern in carry-ing out ISMA on dominant operating cyclic loads typically on practical usage. Low impact forces may not be adequate to excite the structure's natural modes, while excessive impacts may result in non-linearity. Thus, if the information of the cyclic force is known in advance, suitable amount of impact force to be applied on the system can be determined in order to over-

come the dominant cyclic load effect, subsequently all the natural modes in the frequency range of interest are excited.

5. Conclusion

The study has demonstrated the effectiveness of signal attenuation on the response signal where exponential window were applied in the acquired time response signals as well as force screening assessment in the effort of removing the harmonics during ISMA. A combination of exponential windowing with a decay rate of 3 rad/s and applying high impact force which is well below the non-linearity force limit in exciting the structure are favourable in reducing the harmonics to give a better FRF estimation. Thus, the dynamic characteristics of the system and results obtained are comparable with EMA.

Together with the finding in this paper, further works can be proposed to reduce the number of averages (< 250) by investigating another factor which is phase synchronization between acceleration response and response due to cyclic load.

Acknowledgement

The authors wish to acknowledge the financial support and advice given by University of Malaya Research Grant (RP022D-2013AET), Fundamental Research Grant Scheme (FP010-2014A), Postgraduate Research Grant (PG011-2015A), Advanced Shock and Vibration Research (ASVR) Group of University of Malaya and other project collaborators.

References

- [1] N. M. M. Maia and J. M. M. Silva, *Theoretical and Experimental Modal Analysis*, Research Studies Press (1997).
- [2] M. H. Richardson and D. L. Formenti, Parameter estimation from frequency response measurements using rational fraction polynomials, *Proceedings of the 1st International Modal Analysis Conference*, Orlando, Florida, USA (1982) 167-186.
- [3] M. H. Richardson and D. L. Formenti, Global curve fitting of frequency response measurements using the rational fraction polynomial method, *Proceedings of the 3rd International Modal Analysis Conference*, Orlando, Florida, USA (1985) 390-397.
- [4] C. Y. Shih et al., A frequency-domain global parameter-estimation method for multiple reference frequency-response measurements, *Mechanical Systems and Signal Processing*, 2 (4) (1988) 349-365.
- [5] P. Avitabile, Modal space back to basics, *Experimental Techniques*, 35 (1) (2011) 1-2.
- [6] M. M. Fayyadh et al., Combined modal parameters-based index for damage identification in a beamlike structure: theoretical development and verification, *Archives of Civil and Mechanical Engineering*, 11 (3) (2011) 587-609.
- [7] Z. Ismail and Z. C. Ong, Honeycomb damage detection in a reinforced concrete beam using frequency mode shape regression, *Measurement*, 45 (5) (2012) 950-959.
- [8] Z. Ismail, Application of residuals from regression of experimental mode shapes to locate multiple crack damage in a simply supported reinforced concrete beam, *Measurement*, 45 (6) (2012) 1455-1461.
- [9] Z. C. Ong et al., Determination of damage severity on rotor shaft due to crack using damage index derived from experimental modal data, *Experimental Techniques* (2012) (In Press).
- [10] G. H. James et al., The natural excitation technique (Next) for modal parameter extraction from operating structures, *Modal Analysis-the International Journal of Analytical and Experimental Modal Analysis*, 10 (4) (1995) 260-277.
- [11] S. R. Ibrahim and E. C. Mikulcik, The experimental determination of vibration parameters from time responses, *The Shock and Vibration Bulletin*, 46 (5) (1976) 187-196.
- [12] J. N. Juang and R. S. Pappa, An eigensystem realization-algorithm for modal parameter-identification and model-reduction, *Journal of Guidance Control and Dynamics*, 8 (5) (1985) 620-627.
- [13] P. Mohanty and D. J. Rixen, A modified Ibrahim time domain algorithm for operational modal analysis including harmonic excitation, *Journal of Sound and Vibration*, 275 (1-2) (2004) 375-390.
- [14] R. S. Pappa and S. R. Ibrahim, A parametric study of the Ibrahim time domain modal identification algorithm, *The Shock and Vibration Bulletin*, 51 (3) (1981) 43-57.
- [15] R. Brincker et al., Modal identification from ambient responses using frequency domain decomposition, *Proc. of the 18th International Modal Analysis Conference (IMAC)*, San Antonio, Texas (2000).
- [16] B. Schwarz and M. H. Richardson, Modal parameter estimation from ambient response data, *Proceedings of the 19th International Modal Analysis Conference*, Orlando, Florida, USA (2001) 1017-1022.
- [17] B. Schwarz and M. H. Richardson, Using a de-convolution window for operating modal analysis, *Proceedings of the 2nd International Operational Modal Analysis Conference*, Orlando, Florida, USA (2007) 1-7.
- [18] L. M. Zhang et al., Modal indicators for operational modal identification, *Proceedings of the 19th International Modal Analysis Conference*, Orlando, Florida, USA (2001) 746-752.
- [19] D. Kang et al., Phase difference correction method for phase and frequency in spectral analysis, *Mechanical Systems and Signal Processing*, 14 (5) (2000) 835-843.
- [20] X. Ming and D. Kang, Corrections for frequency, amplitude and phase in a fast Fourier transform of a harmonic signal, *Mechanical Systems and Signal Processing*, 10 (2) (1996) 211-221.
- [21] K. Y. Qi, et al., Vibration based operational modal analysis of rotor systems, *Measurement*, 41 (7) (2008) 810-816.
- [22] M. J. Whelan et al., Operational modal analysis of a multi-span skew bridge using real-time wireless sensor networks, *Journal of Vibration and Control*, 17 (13) (2011) 1952-1963.
- [23] A. G. A. Rahman et al., Effectiveness of impact-synchro-

- nous time averaging in determination of dynamic characteristics of a rotor dynamic system, *Measurement*, 44 (1) (2011) 34-45.
- [24] A. G. A. Rahman et al., Enhancement of coherence functions using time signals in modal analysis, *Measurement*, 44 (10) (2011) 2112-2123.
- [25] O. Z. Chao, *Development of impact-synchronous modal analysis technique on motor-driven structure during operation*, Department of Mechanical Engineering, University of Malaya (2013).
- [26] A. G. A. Rahman et al., Impact-synchronous modal analysis (ISMA)- An attempt to find an alternative, *5th International Operational Modal Analysis Conference*, Guimarães, Portugal (2013).
- [27] S. Gade et al., Operational modal analysis on a wind turbine gearbox, *Conference & Exposition on Structural Dynamics* (2009).
- [28] N.-J. Jacobsen et al., Eliminating the influence of harmonic components in operational modal analysis, *Proceedings of The 25th International Modal Analysis Conference (IMAC)* (2007).
- [29] A. G. A. Rahman et al., Enhancement of impact-synchronous modal analysis with number of averages, *Journal of Vibration and Control*, 20 (11) (2014) 1645-1655.
- [30] S. Y. Khoo et al., Impact force identification with pseudo-inverse method on a lightweight structure for under-determined, even-determined and over-determined cases, *International Journal of Impact Engineering*, 63 (2014) 52-62.
- [31] Y. Ding et al., Average acceleration discrete algorithm for force identification in state space, *Engineering Structures*, 56 (2013) 1880-1892.
- [32] C. Ma and H. X. Hua, Force identification technique by the homotopy method, *Journal of Mechanical Science and Technology*, 29 (10) (2015) 4083-4091.
- [33] L. J. Wang et al., A new regularization method and application to dynamic load identification problems, *Inverse Problems in Science and Engineering*, 19 (6) (2011) 765-776.
- [34] A. Brandt, Spectrum and correlation estimates using the DFT, *Noise and Vibration Analysis*, John Wiley & Sons, Ltd. (2011) 205-243.
- [35] D. L. Formenti and M. H. Richardson, Parameter estimation from frequency response measurements using rational fraction polynomials (Twenty Years of Progress), *Proceedings of the 20th International Modal Analysis Conference*, Los Angeles, California, USA (2002) 373-382.
- [36] K. Worden and G. R. Tomlinson, *Nonlinearity in Structural Dynamics: Detection, Identification and Modelling*, Taylor & Francis (2000).
- [37] A. G. A. Rahman, *Dynamic of Machine Structures and Case Studies*, 1st Edition, Unpublished, University of Malaya.



Ong Zhi Chao received his Ph.D. from the University of Malaya, Malaysia. He is currently a Senior Lecturer at the Mechanical Engineering Department, Faculty of Engineering, University of Malaya. His research interests include vibration, modal analysis, impact-synchronous modal analysis (ISMA), structural and rotor dynamics, virtual instrumentation, signal processing, fault diagnostic.



Lim Hong Cheet received his Bachelor Degree of Mechanical Engineering (Honours) from the University of Malaya, Malaysia. He is currently a post-graduate researcher at the Mechanical Engineering Department, Faculty of Engineering, University of Malaya. His research interests include vibration, modal analysis, impact-synchronous modal analysis (ISMA), virtual instrumentation, signal processing.